

## Structure refinement of a synthetic knorringite, $\text{Mg}_3(\text{Cr}_{0.8}\text{Mg}_{0.1}\text{Si}_{0.1})_2(\text{SiO}_4)_3$

AMÉLIE JUHIN,<sup>1,\*</sup> GUILLAUME MORIN,<sup>1</sup> ERIK ELKAÏM,<sup>2</sup> DANIEL J. FROST,<sup>3</sup> MICHEL FIALIN,<sup>4</sup>  
FARID JUILLOT,<sup>1</sup> AND GEORGES CALAS<sup>1</sup>

<sup>1</sup>Institut de Minéralogie et de Physique des Milieux Condensés, Université Paris 6, Université Paris 7, IPGP and CNRS,  
140 rue de Lourmel 75015 Paris, France

<sup>2</sup>Synchrotron SOLEIL, L'Orme des Merisiers, Saint-Aubin, BP 48 91192 Gif-sur-Yvette Cedex, France

<sup>3</sup>Bayerisches Geoinstitut, Universität Bayreuth, D-95440 Bayreuth, Germany

<sup>4</sup>Centre de Microanalyse Camparis-CNRS, Université Paris 6, 4 place Jussieu, 75252 Paris cedex 5, France

### ABSTRACT

The crystal structure of a polycrystalline knorringite,  $\text{Mg}_3(\text{Cr}_{0.8}\text{Mg}_{0.1}\text{Si}_{0.1})_2(\text{SiO}_4)_3$ , synthesized at 11 GPa and  $T = 1500$  °C in a multi-anvil press, has been refined from high-resolution synchrotron X-ray powder diffraction data. The structure is cubic, space group  $Ia\bar{3}d$ ,  $a = 11.5935(1)$  Å,  $V = 1558.27(4)$  Å<sup>3</sup>,  $D_{\text{calc}} = 3.79$  g/cm<sup>3</sup>. The structural formula indicates that knorringite is susceptible to majorite substitution at these synthesis conditions. The Cr-O distance, 1.959(7) Å, is similar to that in Cr-bearing pyrope  $\text{Mg}_3\text{Al}_2(\text{SiO}_4)_3$ . This confirms that the magnitude of the Cr-O distance is not responsible for the difference in crystal field splitting values between green knorringite and red Cr-pyrope. A comparison with the structure of other Cr-garnet end-members shows that the Cr-O distance and the <sup>141</sup>Si-O-Cr angle decrease with decreasing synthesis pressure and with increasing X-cation size.

**Keywords:** Structure refinement, knorringite, XRD, synchrotron powder diffraction, Cr-garnet

### INTRODUCTION

Due to their occurrence in the Earth's upper mantle, silicate garnets play a fundamental role in petrogenetic processes occurring at high pressure and high temperature. The general structural formula can be written as  $\text{X}_3\text{Y}_2(\text{SiO}_4)_3$ , where X and Y refer, respectively, to eightfold- and sixfold-coordinated cations, and Si enters the tetrahedral sites. X sites are occupied by large divalent cations (mostly  $\text{Mg}^{2+}$ ,  $\text{Fe}^{2+}$ ,  $\text{Ca}^{2+}$ , and  $\text{Mn}^{2+}$  in natural garnets), whereas Y sites house smaller trivalent cations ( $\text{Al}^{3+}$ ,  $\text{Fe}^{3+}$ , and  $\text{Cr}^{3+}$ ). Most natural silicate garnets occur in complex solid solutions and have a cubic structure, with space group  $Ia\bar{3}d$  (Novak and Gibbs 1971).

Knorringite,  $[\text{Mg}_3\text{Cr}_2(\text{SiO}_4)_3]$ , the Cr end-member of the pyrope garnet series, is an important component of garnet solid solutions in deeper parts of the upper mantle (Irifune et al. 1982). It often occurs as a major component of kimberlite garnets (Nixon and Hornung 1968) and Cr concentration is used for tracing high-pressure, deep-earth conditions favorable to the formation of diamonds, in which garnets with up to 50% of the knorringite component occur as inclusions. The highest knorringite content known so far for natural garnet inclusions in kimberlitic diamonds is 66.4 mol% (Stachel and Harris 1997). Despite the importance of this component in deeper parts of the upper mantle, the structure of the knorringite end-member has not yet been refined. Some predictions have been derived from the structure of natural garnets using empirical laws involving the radii of the cations (Novak and Gibbs 1971) or by performing least-square refinement of the interatomic distances (Otonello et al. 1996). Recently, first-principles calculations based

on density functional theory have been performed (Milman et al. 2001), but the theoretical structure is in disagreement with these predictions. In particular, the calculated Cr-O distance (1.976 Å) is larger than the two predicted ones (1.958 and 1.960 Å). The uncertainty about the structure of knorringite certainly prevents completion of the investigation of the thermodynamic and structural properties associated with the incorporation of Cr in garnets. For example, in Cr-containing pyrope,  $\text{Cr}^{3+}$  substitutes for  $\text{Al}^{3+}$  in the Y site, and the accommodation of the mismatch leads to a local structural relaxation of the pyrope structure: the Cr-O distance in Cr-containing pyrope is larger by 0.07 Å than the Al-O distance (Juhin et al. 2008), but the determination of how far the structural relaxation goes depends on the value of the Cr-O distance in the knorringite end-member.

The stability field of knorringite has been investigated in several studies (Ringwood 1977; Irifune et al. 1982; Taran et al. 2004; Klemme 2004). Space group ( $Ia\bar{3}d$ ) and lattice parameter [11.600(1) Å, Ringwood 1977; 11.596(1) Å, Irifune et al. 1982] have been determined from X-ray powder diffraction data, but the crystal structure has not yet been refined. In this study, we describe the crystal structure of knorringite with the composition  $\text{Mg}_3(\text{Cr}_{0.8}\text{Mg}_{0.1}\text{Si}_{0.1})_2(\text{SiO}_4)_3$ . The sample was synthesized in a multi-anvil apparatus at  $P = 11$  GPa and  $T = 1500$  °C. Chemical composition was determined using an electron microprobe, and the structure was refined by the Rietveld method, using high-resolution synchrotron X-ray powder diffraction data. Despite a slight amount of majorite component [the tetragonally distorted garnet of composition  $\text{Mg}_3(\text{MgSi})(\text{SiO}_4)_3$ ], the structure is cubic and may be compared to that of other Cr-garnet end-members,  $\text{Ca}_3\text{Cr}_2(\text{SiO}_4)_3$ ,  $\text{Fe}_3\text{Cr}_2(\text{SiO}_4)_3$ , and  $\text{Mn}_3\text{Cr}_2(\text{SiO}_4)_3$ .

\* E-mail: amelie.juhin@impmc.jussieu.fr

## MATERIALS AND EXPERIMENTAL

### High-pressure synthesis

Knorringite was synthesized at high temperature and high pressure at the Bayerisches Geoinstitut (University of Bayreuth, Germany). The starting mixture (i.e., a stoichiometric mixture of dried MgO, Cr<sub>2</sub>O<sub>3</sub>, and noncrystalline SiO<sub>2</sub> plus 1 μL of water) was encapsulated in a Re capsule, which was enclosed in the high-pressure cell of an octahedral multianvil apparatus. The two synthesis runs were performed using a 1000 ton press and a 14 mm edge length MgO octahedral assembly and employing 8 mm truncation edge length tungsten carbide cubes. The samples were heated using a LaCrO<sub>3</sub> furnace, and the temperature was controlled to ±1 °C using a W3%Re/W25%Re thermocouple. Run conditions, which are reported in Table 1, are close to those of Taran et al. (2004) and Klemme (2004). The experimental calibrated pressures are given ±0.3 GPa. The samples were quenched by switching off the power of the furnace, with a quench rate >200 °C/s. Run products were examined for homogeneity under a binocular microscope. To get a rough estimate of their phase composition, powder X-ray diffraction patterns were recorded using a PANalytical X'Pert Pro MPD diffractometer with CuKα radiation. In both samples, referred to as Kn-1 and Kn-2, knorringite was found to be the major phase, associated with a small (similar) amount of eskolaite (α-Cr<sub>2</sub>O<sub>3</sub>) and traces of stishovite (SiO<sub>2</sub>).

### Electron microprobe analysis (EMPA)

The chemical composition of the Kn-1 sample was determined using a CAM-ECA SX50 microprobe at the CAMPARIS center. For this purpose, the ground

**TABLE 1.** Conditions and results of high-pressure multianvil runs

Run no.	Label	P (GPa)	T (°C)	Duration (h)	Appearance	Phases
H2732	Kn-1	11	1500	5	Dark green	Kn + Es (+St)
H2733	Kn-2	14	1600	6	Dark green	Kn + Es (+St)

Notes: Kn represents knorringite, Es eskolaite, and St stishovite. The run numbers are those of the diary of the Bayerisches Geoinstitut.

powder was deposited on a carbon tape and covered with a thin carbon deposit. The probe was operated at 15 kV and 40 nA. Intensities of the Kα emission lines were collected for 10 s per element, using a single spectrometer with a PET analyzing crystal for Si, Mg, and a TAP analyzing crystal for Cr. The same setup was used for collecting data on appropriate standards. This method limited the bias arising from detecting the X-ray emission with different angles when using distinct spectrometers on a non-polished sample. Most of the grains in the ground powder were below 5 μm in size. However, averaging 22 independent analyses on different knorringite grains with sizes ranging from 10 to 20 μm yielded a statistically reliable structural formula.

### X-ray powder diffraction using synchrotron radiation

A high-resolution X-ray powder diffraction pattern of the synthetic Kn-1 sample was recorded in 3 h in transmission Debye-Scherrer geometry at the CRISTAL undulator beamline at the SOLEIL Synchrotron Facility, Saclay, France. Approximately 10 mg of sample were mounted in a rotating silica capillary 300 μm in diameter. The pattern was recorded within the 6–60° (2θ) range with a wavelength of 0.7285 Å. The diffracted beam was collected using a 12 crystal Si(111) analyzer leading to an instrumental peak width lower than 0.01° (2θ), which was evaluated by recording a few Bragg peaks of the LaB<sub>6</sub> powder diffraction standard.

## RESULTS AND DISCUSSION

### Chemical composition

The average of the 22 EPMA analyses provides the following composition: 42.5 (0.6) wt% SiO<sub>2</sub>, 28.8 (0.5) wt% MgO, and 28.6 (0.5) wt% Cr<sub>2</sub>O<sub>3</sub>. The structural formula was then determined as Mg<sub>3</sub>(Cr<sub>0.82</sub>Mg<sub>0.105</sub>Si<sub>0.105</sub>)<sub>2</sub>(SiO<sub>4</sub>)<sub>3</sub>, by assuming that the dodecahedral X site and the tetrahedral site are fully occupied by Mg and Si atoms, respectively.

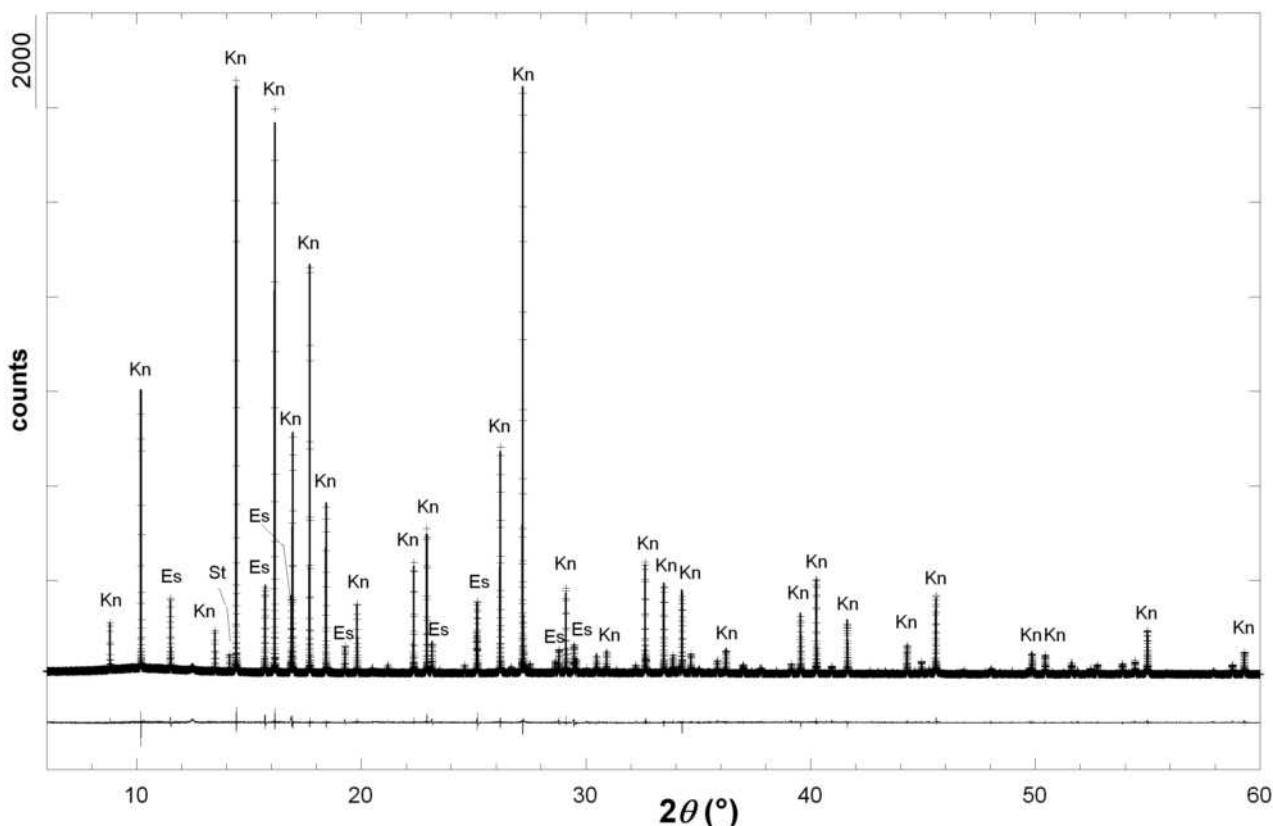


**FIGURE 1.** Rietveld refinement of the X-ray powder pattern of the knorringite sample. Experimental data (crosses), calculated (solid line), difference (thin solid lines). The main Bragg reflections of knorringite (Kn), eskolaite (Es), and stishovite (St) are indicated.

**TABLE 2.** Structure-refinement parameters for knorringite

Formula	Mg <sub>3</sub> (Cr <sub>0.84</sub> Mg <sub>0.08</sub> Si <sub>0.08</sub> ) <sub>2</sub> (SiO <sub>4</sub> ) <sub>3</sub>
Formula weight (g/mol)	444.91
No. of structural formula in cell unit	8
Space group	<i>Ia</i> $\bar{3}d$
<i>a</i> (Å)	11.5935(1)
Unit-cell volume, <i>V</i> (Å <sup>3</sup> )	1558.27(4)
Temperature	ambient
Wavelength (Å)	0.7285
Step increment (2θ)	0.0015
Geometry	Debye-Scherrer
Background	spline
Profile function	pseudo-Voigt
Pattern range (2θ)	6–60
Number of reflections	174
Refined parameters	19
<i>R</i> <sub>wp</sub> (%) overall	12.5
<i>R</i> <sub>p</sub> (%) overall	8.8
Goodness of fit overall	1.11
<i>R</i> <sub>Bragg</sub> (%)	4.7

### Structure refinement

Rietveld refinement was performed on synchrotron X-ray powder-diffraction data in the range 6–60° (2θ), using the program XND (Berar and Baldinozzi 1998). Absorption for Debye-Scherrer geometry (Rouse et al. 1970) was negligible for  $\mu_r = 0.3$  (assuming that the apparent density of the powder would be half that of the mineral). Scale factors, cell parameters, and width and shape parameters of pseudo-Voigt line-profile functions were refined for knorringite Mg<sub>3</sub>Cr<sub>2</sub>Si<sub>3</sub>O<sub>12</sub>, eskolaite α-Cr<sub>2</sub>O<sub>3</sub>, and stishovite SiO<sub>2</sub>. Atom parameters of these two latter phases were kept fixed at the literature values (Newnham and deHaan 1962; Ross et al. 1990). Quantitative analysis derived from scale-factor values, using the classical method without internal standard (Bish and Post 1989) indicated that the eskolaite and stishovite weight fractions in the sample were 10 ± 2 and ~1 wt%, respectively. For knorringite, all atom positions and displacement parameters were refined, together with site occupancies of the cations, using the predicted structure (Novak and Gibbs 1971) as a starting model. About 174 Bragg reflections from knorringite were fit in the 6–60° (2θ) range, and the *R*<sub>wp</sub> parameter for the pattern and the *R*<sub>Bragg</sub> parameter for knorringite reached final values of 0.125 and 0.047, respectively (Fig. 1; Table 2). Refined atomic positions, displacement parameters, and site occupancies are reported in Table 3. The Rietveld refined composition of synthetic knorringite was Mg<sub>3</sub>(Cr<sub>0.84</sub>Mg<sub>0.08</sub>Si<sub>0.08</sub>)<sub>2</sub> (SiO<sub>4</sub>)<sub>3</sub>, in very good agreement with the one determined from EMPA. Within respective experimental uncertainties, this yields an average composition of Mg<sub>3</sub>(Cr<sub>0.8</sub>Mg<sub>0.1</sub>Si<sub>0.1</sub>)<sub>2</sub>(SiO<sub>4</sub>)<sub>3</sub>. This result will be discussed later in the paper.

The Rietveld-refined cell parameter *a* [11.5935(1) Å] is in good agreement with previous experimental values obtained for knorringite, 11.600 Å (Ringwood 1977), 11.596(1) Å (Irifune et al. 1982), and 11.5954(5) Å (Taran et al. 2004), and also with the 11.6040 Å value calculated by Ottonello et al. (1996). The Rietveld-refined Cr-O distance [1.959(7) Å] is close to the values of 1.958 and 1.960 Å predicted by Novak and Gibbs (1971) and Ottonello et al. (1996), respectively, on the basis of a least-squares refinement procedure on a series of natural samples. However, it is significantly shorter than the Cr-O distance derived from a first-principles calculation (1.976 Å, Milman et al. 2001), which may be explained by an overestimation of the cell

**TABLE 3.** Atomic parameters for knorringite: fractional coordinates, isotropic Debye-Waller factor (*B*<sub>iso</sub>), occupancy factor (Occ), and site multiplicity (Mult)

Atom	<i>x/a</i>	<i>y/b</i>	<i>z/c</i>	<i>B</i> <sub>iso</sub> (Å <sup>2</sup> )	Occ	Mult
Cr <sup>3+</sup>	0	0	0	0.34(3)	0.84(2)*	16
Mg <sup>2+</sup>	0	0	0	–	0.08(2)*	–
Si <sup>4+</sup>	0	0	0	–	0.08(2)*	–
Mg <sup>2+</sup>	1/8	0	1/4	1.12(6)	1	24
Si <sup>4+</sup>	3/8	0	1/4	0.46(2)	1	24
O <sup>2-</sup>	0.0348(2)	0.0516(2)	0.6571(2)	1.08(6)	1	96

Notes: Standard deviations on the last digit are under brackets. “–” indicates a value identical to that above it in the table.

\* Occupancy factors refined with the following constraint on the octahedral site: Occ(Mg<sup>2+</sup>) = Occ(Si<sup>4+</sup>) = 1 – Occ(Cr<sup>3+</sup>), which satisfies electro-neutrality of the substitution.

**TABLE 4.** Selected distances (Å) and angles (°) in CrO<sub>6</sub>/MgO<sub>6</sub>/SiO<sub>4</sub> polyhedra for knorringite

	Distance (Å)	Angle (°)
Cr-O	1.959(7) × 6	
O-O (unshared)	2.811(7) × 6	91.7(1)
O-O (Mg-shared)	2.729(7) × 6	88.3(1)
Si-O	1.616(8) × 4	
O-O (Mg-shared)	2.464(7) × 2	99.3(1)
O-O (unshared)	2.722(7) × 4	114.7(1)
Mg-O <sub>a</sub>	2.225(6) × 4	
Mg-O <sub>b</sub>	2.365(6) × 4	
O <sub>a</sub> -O <sub>a</sub> (Si-shared)	2.464(7) × 2	67.2(1)
O <sub>a</sub> -O <sub>b</sub> (Cr-shared)	2.729(7) × 4	72.9(1)
O <sub>b</sub> -O <sub>b</sub> (unshared)	2.784(8) × 2	72.1(1)
O <sub>a</sub> -O <sub>b</sub> (Mg-shared)	2.698(7) × 4	71.9(1)
Cr-Cr	5.020 (7) × 6	

Note: Standard deviations on the last digit are in parentheses.

parameter *a* (11.646 Å). The (Cr/Mg)-Si distance [3.240(6) Å] determined from the present Rietveld analysis is close to both the distances predicted by Novak and Gibbs (1971) (3.253 Å) and Ottonello et al. (1996) (3.243 Å), and to the theoretical one derived from first-principles calculation (3.255 Å, Milman et al. 2001). The values of other selected interatomic distances and angles are reported in Table 4. Using these structural data, we have performed a bond-valence analysis using the Chardi (or CD) method (Hoppe et al. 1989), which, in the case of mixed cation occupancies, is known to provide better results than the classical bond-valence approach of Brown and Altermatt (1985). The effective coordination numbers (ECoN) and bond-valence sums (BV) were calculated using the CHARDI-IT program (Nespolo et al. 2001), which uses an iterative procedure to calculate the charge distribution. We found that the Mg ions entering the X site have an ECoN of 7.74 and a BV of 2.0. The ECoN for Mg is slightly different from 8.0, since the X site is highly distorted. The fourfold-coordinated Si ions have an ECoN of 4.0 and a BV of 4.0. The octahedral site, which is occupied by Cr, Si, and Mg ions, has an ECoN of 6.0 and a BV of 3.0. All O atoms have a BV of 2.0. These results indicate that the refined structure of the synthetic knorringite sample is valence-balanced and correct.

### Implications for Cr<sup>3+</sup> crystal chemistry in Mg-garnets

Chromium-bearing pyrope is an important mineral of the lithospheric upper mantle. In this mineral, Cr concentration increases with depth and thus is used in mantle barometry (Grütter et al. 2006). Also, when Cr is present in the garnet lattice, the spinel-garnet transformation is shifted significantly to pressures as high as 7 GPa (Klemme 2004). The modeling

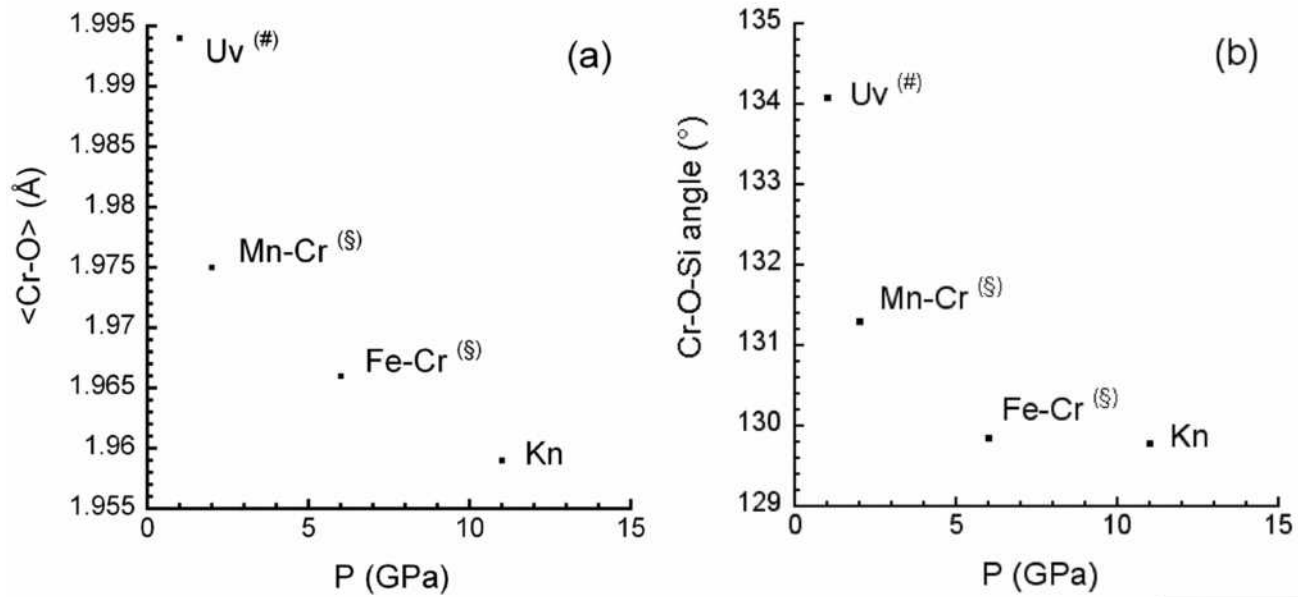


**FIGURE 2.** (a) Dependence of  $\langle\text{Cr-O}\rangle$  distance (Å) on minimum pressure of synthesis (GPa) for Cr-garnet end-members. (b) Dependence of Cr-O-Si angle (°) on pressure of synthesis (GPa). Uv =  $\text{Ca}_3\text{Cr}_2(\text{SiO}_4)_3$ , Mn-Cr =  $\text{Mn}_3\text{Cr}_2(\text{SiO}_4)_3$ , Fe-Cr =  $\text{Fe}_3\text{Cr}_2(\text{SiO}_4)_3$ , and Kn =  $\text{Mg}_3\text{Cr}_2(\text{SiO}_4)_3$ ; # = Andrut and Wildner (2002), § = calculated from Ottonello et al. (1996).

of thermodynamic properties thus requires a careful investigation of the local structural rearrangements occurring along the solid solution. The Cr-O distance in natural Cr-bearing pyrope, determined by EXAFS measurements and ab initio calculations as  $1.96 \pm 0.01$  Å (Juhin et al. 2008), is identical to the Cr-O distance in the  $\text{Mg}_3(\text{Cr}_{0.8}\text{Mg}_{0.1}\text{Si}_{0.1})_2(\text{SiO}_4)_3$  structure refined in this study, within experimental uncertainties. The local crystallographic structure around substitutional  $\text{Cr}^{3+}$  predicted by ab initio calculations on pyrope is also similar to that around  $\text{Cr}^{3+}$  in  $\text{Mg}_3(\text{Cr}_{0.8}\text{Mg}_{0.1}\text{Si}_{0.1})_2(\text{SiO}_4)_3$ . This confirms that the Al-Cr substitution in pyrope is accompanied by a full relaxation of the oxygen first neighbors in the Y site. Despite different Cr-O distances, a similar full relaxation exists in Cr-dilute spinel (Juhin et al. 2007). A second conclusion concerns the origin of the color differences between Mg-garnets: the difference in crystal-field splitting ( $\Delta_o$ ) values between red Cr-pyrope and green knorringite (Taran et al. 2004) cannot be attributed to the variation of the Cr-O distance in a point-charge model ( $\Delta_o \propto \langle\text{Cr-O}\rangle^{-5}$ , Burns 1993). Such a difference may be rather related to changes in the electronic structure of the octahedral  $[\text{Cr}^{3+}\text{O}_6]$  site, i.e., Cr-O bond covalency and effective charge of the O ligands. This is in line with previous results obtained on  $\alpha\text{-Al}_2\text{O}_3\text{:Cr}^{3+}$  and  $\alpha\text{-Cr}_2\text{O}_3$  (Gaudry et al. 2006), which confirms the role of the Cr-O bond in the variation of  $\Delta_o$ .

#### Comparison between the crystal structure of high-pressure Cr-garnet end-members

The increasing pressure of formation for Cr-garnet end-members seems to be related to the decrease in the ionic radius of the dodecahedral divalent cation [ $r(\text{Ca}^{2+}) = 1.12$  Å,  $r(\text{Mn}^{2+}) = 0.96$  Å,  $r(\text{Fe}^{2+}) = 0.92$  Å, and  $r(\text{Mg}^{2+}) = 0.89$  Å] (Fursenko 1981). Indeed, uvarovite [ $\text{Ca}_3\text{Cr}_2(\text{SiO}_4)_3$ ] is formed at ambient pressure (Andrut and Wildner 2002), other Cr-garnet end-members,  $\text{Mn}_3\text{Cr}_2(\text{SiO}_4)_3$  and  $\text{Fe}_3\text{Cr}_2(\text{SiO}_4)_3$ , are synthesized above  $P \sim 2$

and  $\sim 5\text{--}6$  GPa, respectively (Fursenko 1981; Woodland et al. 2009), which is consistent with  $\text{Mg}_3\text{Cr}_2(\text{SiO}_4)_3$  being stable above  $P \sim 11$  GPa (Irifune et al. 1982). Although the crystal structures of  $\text{Mn}_3\text{Cr}_2(\text{SiO}_4)_3$  and  $\text{Fe}_3\text{Cr}_2(\text{SiO}_4)_3$  have not yet been refined, they have been predicted (Novak and Gibbs 1971; Ottonello et al. 1996). The respective lattice parameters are in good agreement with the values measured from X-ray powder diffraction data (Fursenko 1981). Since the predicted interatomic distances of knorringite are similar to the ones we determined by Rietveld refinement, we can infer that the predictions made for the structures of  $\text{Mn}_3\text{Cr}_2(\text{SiO}_4)_3$  and  $\text{Fe}_3\text{Cr}_2(\text{SiO}_4)_3$  also yield valuable information. Therefore, we used the predicted structures given by Ottonello et al. (1996) for these two garnets and the refined structures of  $\text{Ca}_3\text{Cr}_2(\text{SiO}_4)_3$  (Andrut and Wildner 2002) and  $\text{Mg}_3\text{Cr}_2(\text{SiO}_4)_3$  to better understand the effect of pressure on structural changes in these garnet series. The evolution of the Cr-O distance and the  $^{14}\text{Si-O-Cr}$  angle, together with the minimum pressure of synthesis, is plotted in Figures 2a and 2b, respectively. The Cr-O distance decreases as synthesis pressure increases, showing a significant compression of the  $\text{CrO}_6$  octahedron. Additionally, the  $^{14}\text{Si-O-Cr}$  angle decreases by 3.7% from uvarovite to knorringite, while at the same time, the  $^{14}\text{Si-O}$  distance decreases by 1.5% [ $\langle^{14}\text{Si-O}\rangle = 1.6447$  Å in  $\text{Ca}_3\text{Cr}_2(\text{SiO}_4)_3$  vs.  $\langle^{14}\text{Si-O}\rangle = 1.620$  Å in  $\text{Mg}_3\text{Cr}_2(\text{SiO}_4)_3$ ]. This confirms the early predictions made by Fursenko (1981) and shows that the compression of the garnet structure is achieved by the rotation of  $\text{SiO}_4$  tetrahedra with respect to  $\text{CrO}_6$  octahedra, rather than by their deformation (Ungaretti et al. 1995).

Despite recent investigations on the crystal chemistry of Fe-knorringite (Woodland et al. 2009), a structure refinement of  $\text{Mn}_3\text{Cr}_2(\text{SiO}_4)_3$  and  $\text{Fe}_3\text{Cr}_2(\text{SiO}_4)_3$  is needed to quantify the structural stability of Cr-garnets at high pressure and temperature. Moreover, the study of  $\text{A}_3\text{Cr}_2(\text{SiO}_4)_3\text{--B}_3\text{Cr}_2(\text{SiO}_4)_3$  and  $\text{A}_3\text{Al}_2(\text{SiO}_4)_3\text{--A}_3\text{Cr}_2(\text{SiO}_4)_3$  joins (with A, B = Ca, Mn, Fe,

Mg) could provide valuable information for understanding the mechanisms prevailing at the incorporation of Cr in garnets, and their significance in samples recovered from the lithospheric upper mantle.

### A majoritic component in synthetic knorringite

The structural formula obtained from EMPA and the Rietveld refinement,  $\text{Mg}_3(\text{Cr}_{0.8}\text{Mg}_{0.1}\text{Si}_{0.1})_2(\text{SiO}_4)_3$ , shows that a small amount of Mg and Si are incorporated in the Y site. We have checked that starting from a stoichiometric mixture of oxides, the amount of Cr missing in the octahedral site is actually consistent with the proportion of  $\alpha\text{-Cr}_2\text{O}_3$  obtained as a side product. Our results indicate that knorringite is susceptible to majorite substitution within the experimental conditions used in this work ( $P = 11$  GPa,  $T = 1500$  °C, and run duration of 5 to 6 h). This behavior is similar to that observed for pyrope at lower pressures (Ringwood 1967; Liu 1977). However, Klemme (2004) reported the absence of a majorite component (within the uncertainties of microprobe analysis) at higher pressure ( $P = 16$  GPa,  $T = 1600$  °C) and similar run durations, suggesting a different behavior of pyrope and knorringite with respect to the extent of majorite substitution. Our findings suggest that these differences may indeed be dependent on synthesis conditions because garnets nucleate sluggishly at high pressure. Owing to the importance of the activity of majorite in garnets in understanding the formation and evolution of rocks from the deep upper mantle (see, e.g., Scambelluri et al. 2008), further investigations are needed to understand the extent of majorite substitution in knorringite as a function of pressure and temperature.

### ACKNOWLEDGMENTS

The authors are grateful to G. Gudfinnsson for help in the preparation of the high-pressure synthesis runs. These experiments were performed at the Bayerisches Geoinstitut under the EU "Research Infrastructures: Transnational Access" Program [contract no. 505320 (RITA)-High Pressure]. This is IPGP contribution no. 2562.

### REFERENCES CITED

- Andrut, M. and Wildner, M. (2002) The crystal chemistry of birefringent natural uvarovites. Part III. Application of the superposition model of crystal fields with a characterization of synthetic cubic uvarovite. *Physics and Chemistry of Minerals*, 29, 595–608.
- Berar, J.F. and Baldinozzi, G. (1998) XND code: From X-ray laboratory data to incommensurately modulated phases. Rietveld modeling of complex materials. *International Union of Crystallography—Commission for Powder Diffraction Newsletter*, 20, 3–5.
- Bish, D.L. and Post, J.E. (1989) Reitveld refinement of crystal structures using powder X-ray diffraction data. In D.L. Bish and J.E. Post, Eds., *Modern Powder Diffraction*, 20, p. 277–308. *Reviews in Mineralogy*, Mineralogical Society of America, Chantilly, Virginia.
- Brown, I.D. and Altermatt, D. (1985) Bond-valence parameters obtained from a systematic analysis of the inorganic crystal structure database. *Acta Crystallographica*, B41, 244–247.
- Burns, R.G. (1993) *Mineralogical Applications of Crystal Field Theory*, 2nd edition, 574 p. Cambridge University Press, U.K.
- Fursenko, B.A. (1981) Synthesis of new high pressure garnets:  $\text{Mn}_3\text{Cr}_2\text{Si}_3\text{O}_{12}$  and  $\text{Fe}_3\text{Cr}_2\text{Si}_3\text{O}_{12}$ . *Bulletin de Minéralogie*, 104, 418–422.
- Gaudry, E., Sainctavit, Ph., Juillot, F., Bondioli, F., Ohresser, Ph., and Letard, I. (2006) From the green color of eskolaite to the red color of ruby: An X-ray absorption spectroscopy study. *Physics and Chemistry of Minerals*, 32, 710–720.
- Grütter, H., Latti, D., and Menzies, A. (2006) Cr-saturation in concentrate garnet compositions from kimberlite and their use in mantle barometry. *Journal of Petrology*, 47, 801–820.
- Hoppe, R., Voigt, S., Glaum, H., Kissel, J., Müller, H.P., and Bernet, K. (1989) A new route to charge distributions in ionic solids. *Journal of the Less-Common Metals*, 156, 105–122.
- Irifune, T., Ohtani, E., and Kumozawa, M. (1982) Stability field of knorringite  $\text{Mg}_3\text{Cr}_2\text{Si}_3\text{O}_{12}$  at high pressure and its implication to the occurrence of Cr-rich pyrope in the upper mantle. *Physics of the Earth and Planetary Interiors*, 27, 263–272.
- Juhin, A., Calas, G., Cabaret, D., Galois, L., and Hazemann, J.L. (2007) Structural relaxation around substitutional  $\text{Cr}^{3+}$  in  $\text{MgAl}_2\text{O}_4$ . *Physical Review B*, 76, 054105.
- (2008) Structural relaxation around substitutional  $\text{Cr}^{3+}$  in pyrope garnet. *American Mineralogist*, 93, 800–805.
- Klemme, S. (2004) The influence of Cr on the garnet-spinel transition in the Earth's mantle: Experiments in the system  $\text{MgO-Cr}_2\text{O}_3\text{-SiO}_2$  and thermodynamic modeling. *Lithos*, 77, 636–646.
- Liu, L. (1977) The system enstatite-pyrope at high pressures and temperatures and the mineralogy of the Earth's mantle. *Earth and Planetary Science Letters*, 36, 237–245.
- Milman, V., Akhmatkaya, E.E., Nobes, R.H., Winkler, B., Pickard, C.J., and White, J.A. (2001) Systematic *ab initio* study of the compressibility of silicate garnets. *Acta Crystallographica*, B57, 163–177.
- Nespolo, M., Ferraris, G., Ivaldi, G., and Hoppe, R. (2001) Charge distribution as a tool to investigate structural details. II. Extension to hydrogen bonds, distorted, and hetero-ligand polyhedra. *Acta Crystallographica B*, 57, 652–664.
- Newham, R.E. and deHaan, Y.M. (1962) Refinement of the  $\alpha\text{-Al}_2\text{O}_3$ ,  $\text{Ti}_2\text{O}_3$ ,  $\text{V}_2\text{O}_5$ , and  $\text{Cr}_2\text{O}_3$  structures. *Zeitschrift für Kristallographie*, 117, 235–237.
- Nixon, P.H. and Hornung, G. (1968) A new chromium garnet end-member, knorringite, from kimberlite. *American Mineralogist*, 53, 1833–1840.
- Novak, G.A. and Gibbs, G.V. (1971) The crystal chemistry of the silicate garnets. *American Mineralogist*, 56, 791–825.
- Ottonello, G., Bokreta, M., and Sciuto, P.F. (1996) Parametrization of energy and interaction in garnets: End-member properties. *American Mineralogist*, 81, 429–447.
- Ringwood, A.E. (1967) The pyroxene garnet transformation in the Earth's mantle. *Earth and Planetary Science Letters*, 2, 255–263.
- (1977) Synthesis of pyrope-knorringite solid solution series. *Earth and Planetary Science Letters*, 36, 443–448.
- Ross, N.L., Shu, J.-F., Hazen, R.M., and Gasparik, T. (1990) High-pressure crystal chemistry of stishovite. *American Mineralogist*, 75, 739–747.
- Rouse, K.D., Cooper, M.J., York, E.J., and Chakera, A. (1970) Absorption correction for neutron diffraction. *Acta Crystallographica*, A26, 682–691.
- Scambelluri, M., Petke, T., and van Roermund, H.L.M. (2008) Majoritic garnets monitor deep subduction fluid flow and mantle dynamics. *Geology*, 36, 59–62.
- Stachel, T. and Harris, J.W. (1997) Syngenetic inclusions in diamond from the Birim field (Ghana)—a deep peridotitic profile with a history of depletion and re-enrichment. *Contributions to Mineralogy and Petrology*, 127, 336–352.
- Taran, M.N., Langer, K., Abs-Wurmbach, I., Frost, D.J., and Platonov, A.N. (2004) Local relaxation around  $^{60}\text{Cr}^{3+}$  in synthetic pyrope-knorringite garnets,  $^{18}\text{Mg}_3\text{[}^{60}(\text{Al}_{1-x}\text{Cr}_x\text{)}_2\text{]Si}_3\text{O}_{12}$ , from electronic absorption spectra. *Physics and Chemistry of Minerals*, 31, 650–657.
- Ungaretti, L., Leona, M., Merli, M., and Oberti, R. (1995) Non-ideal solid solutions in garnet: crystal-structure evidence and modeling. *European Journal of Mineralogy*, 7, 1299–1312.
- Woodland, A.B., Bauer, M., Boffa-Ballaran, T., and Hanrahan, M. (2009) Crystal chemistry of  $\text{Fe}_3^{2+}\text{Cr}_2\text{Si}_3\text{O}_{12}$ – $\text{Fe}_3^{2+}\text{Fe}_3^{3+}\text{Si}_3\text{O}_{12}$  garnet solid solutions and related spinels. *American Mineralogist*, 94, 359–366.

MANUSCRIPT RECEIVED MARCH 14, 2009

MANUSCRIPT ACCEPTED AUGUST 19, 2009

MANUSCRIPT HANDLED BY IAN SWAINSON